PHYSICAL REVIEW B VOLUME 6, NUMBER 8 15 OCTOBER 1972

Measurement and Analysis of the Isotope-Induced One-Phonon Infrared Absorption in LiF†

J. E. Eldridge
Department of Physics, University of British Columbia, Vancouver 8, British Columbia, Canada
(Received 17 April 1972)

Measurements of the far-infrared isotope-induced one-phonon absorption in single-crystal natural lithium fluoride at approximately 10 °K are reported. The main feature observed shows a decrease in the frequency of the [100] transverse acoustic (TA) branch at X_5' of (2–3)% compared with the room-temperature value measured by inelastic neutron scattering. The measured absorption constant agrees poorly with that predicted using the modified deformation-dipole data of Karo and Hardy, but agrees very well with that predicted by the shell model fitted to the measured dispersion curves. An intensity discrepancy, as the feature due to X_5' is approached, indicates an error, however, in the shell-model lithium-ion eigenvectors along the [100] TA direction of up to (15 ± 5)%. The shell-model data have also been used to calculate the contribution of the isotope-induced one-phonon processes to the measured conductivity above the reststrahlen frequency. It is seen that this contribution may explain some of the minor features observed in that region.

I. INTRODUCTION

Infrared absorption by single phonons in pure alkali halides is limited by momentum conservation to the strong "reststrahlen" absorption by the transverse optic (TO) branch near zero wave vector $\vec{k}$. Two-phonon sum and difference processes with near-zero resultant wave vector are observed, with less intensity, on either side of the reststrahlen peak, as also are very weak higher-order-phonon processes satisfying the momentum requirements. The introduction of monovalent impurities into the lattice destroys the lattice periodicity and relaxes the condition of momentum conservation by the lattice phonons. One-phonon band absorption reflecting the density of phonon states may then be directly observed, as well as possible local modes and in-band resonances, depending on the impurity. Chemical impurities experience a potential appreciably different from that of the replaced host ion, so that complex force models must be used to calculate the single-phonon absorption.[1] Isotopic impurities, however, act as weakly perturbing mass defects which if present in sufficient concentration produce in the far infrared a measurable one-phonon absorption band which is directly proportional to the weighted density of states of the isotope ion. This absorption falls off in a Lorentzian fashion away from the reststrahlen frequency, since the transverse optic mode ($\vec{k} \simeq 0$) is the mode driven by the radiation. Macdonald, Klein, and Martin[2] measured the far-infrared absorption produced by monovalent impurities in sodium chloride, including the natural Cl^{37} (24.5%) isotope. The comparison of the isotopic-impurity absorption with theory, using a shell model to generate the host lattice phonons, was excellent and they were able to suggest probable critical-point assignments to the two main features. Their main adjustable parameter appeared to be the effective charge associated with the host-ion motions. No mention was made, however, of the possible errors in the Cl eigenvectors which are used to weight the Cl-ion density of states. Recently, Reid[3] has shown that different lattice-dynamical models, which fit neutron-measured dispersion curves well, can differ appreciably in the ratio of the separate ion eigenvectors in symmetry directions. Measurements to 1% accuracy of the inelastic single-phonon scattering of x rays are predicted to be capable of discriminating between these models. If, however, the effective charge is known well, then the isotope-induced one-phonon infrared absorption should be able to measure more easily the eigenvectors of the isotope ion, which automatically gives the eigenvector for the other ion. This will be possible for only a few symmetry points, for which absorption is not forbidden by symmetry, and which have frequencies not too much below the reststrahlen frequency, so that the intensity is not too weak.

Measurements have therefore been made and are here presented of the one-phonon absorption in natural LiF induced by the Li^6 isotope (7.5%), from 140 to 300 cm^{-1}. The absorption has been compared with the theory from Ref. 2 using both the modified deformation-dipole data of Karo and Hardy and the Li-ion weighted density of states (frequency distribution curves) obtained by Dolling *et al.*[4] from their shell model fitted to dispersion curves which had been measured by inelastic neutron scattering. The deformation-dipole model deviates somewhat from the measured dispersion curves and has already been found by the author[5] to predict two-phonon absorption peaks away from experimental points. Consequently, the agree-

ment with the neutron-fitted data is superior and is in fact generally excellent. The discrepancy in one region, however, is thought to be outside experimental error and to be due to errors in the eigenvectors near the zone boundary. The absorption measurements have been used to calculate the low-frequency Li-ion density of states.

Both the measurements reported here and in Ref. 2 were performed at low temperatures so that the two-phonon difference absorption which occurs predominantly below the reststrahlen frequency is negligible. The two-phonon summation absorption remains finite and indeed very strong at low temperatures, so that it has been thought to obscure any weak isotope-induced absorption above the reststrahlen peak. Using the Dolling density of Li states, however, a calculation of the isotope-induced conductivity has been made in the high-frequency region. Although this one-phonon contribution rapidly falls to a very small fraction of the total as the frequency is increased, it is thought to be responsible for some of the features in the measured conductivity spectrum.

II. EXPERIMENTAL PROCEDURE AND RESULTS

The measurements were performed with an RIIC FS 720 Fourier spectrophotometer, with a step drive and Golay detector. The noise from the detector put a limit on the resolution obtainable in the high-frequency region, just below the reststrahlen frequency of 318 cm^{-1}, where the absorption was rising rapidly. It also contributed to the large error bars in the low-frequency region where the absorption was very small. Black polyethylene and a thick CsI filter (with a 6-μ Mylar beam splitter) were used to restrict the spectral range for measurements near 300 cm^{-1}. A Beckman filter No. 2. (cutoff at 220 cm^{-1}) with a 12-μ beam splitter was used for measurements near 150 cm^{-1}. The resolution was approximately 8 cm^{-1} after apodization (which considerably reduced the noise). The samples were attached to a copper cold finger, which was cooled by liquid helium, and could be rotated to insert one of two samples in the beam or allow the beam to pass unattenuated (the "reference" spectrum). Collimating slits to reduce divergence effects and to ensure that the beam size was the same for the reference and sample runs were positioned on the nitrogen jacket surrounding the samples. There are two effects resulting from the use of a converging or diverging beam. One is that the extreme rays travel further than the thickness d of the sample. The other is a shift in the focus. The first effect is to give larger values of α than the true value. The second effect works in the same direction if the detector is set at the focus. In the present case, however, the focus is normally in the center of the sample chamber some distance from the detector, which is fitted with a black polyethylene lens to converge the beam into a light pipe. The samples on the cold finger could be placed just before or just after the focus (both of which positions shift the focus, real in the first case, apparent in the second, towards the detector), and thus the measured α would be below the true value. Therefore no measurements or corrections were made: The divergence was reduced by the slits and the effects were presumed to be small and to partially cancel each other. The temperature of the samples was approximately 10 °K.

The natural LiF single crystals were obtained from Harshaw Chemical Company, cut with a diamond saw, mechanically polished with alumina on a Nylon cloth with alumina sizes diminishing to 0.3 μ, and finally ultrasonically cleaned. The final sample size was approximately 1×2.5 cm with approximate thicknesses of 0.8, 0.1, and 0.02 cm.

Even though the temperature was low enough to reduce the two-phonon absorption to a negligible amount, it was not known how far into the low-energy region the two-phonon summation processes extended. Earlier calculations[5] with the deformation-dipole data of Karo and Hardy had indicated appreciable absorption down to 250 cm^{-1}. Samples of isotopically pure Li^7F were therefore purchased from Harshaw, with thicknesses close to those above, but having been already polished. A ratio was made of the intensities transmitted through both the pure and impure samples with the reference intensity I_0, in order to calculate both of the absorption coefficients α_{pure} and α_{imp}. These were obtained from the following equation:

$$I=\frac{I_0(I-R)^2\, e^{-\alpha d}}{1-R^2\, e^{-2\alpha d}}, \tag{1}$$

where d is the sample thickness and R is the power reflectance, given for normal incidence by

$$R=(n-1)^2/(n+1)^2 \tag{2}$$

if the extinction coefficient is small, which was the case. The refractive index n was calculated from the classical dispersion formula

$$n^2=\epsilon_\infty+\frac{(\epsilon_0-\epsilon_\infty)}{1-\omega^2/\omega_0^2}. \tag{3}$$

The values for ϵ_∞, ϵ_0, and ω_0 at 2 °K were taken from Lowndes and Martin[6] and may be seen in Table I. Equation (1) assumes an averaging of the multiple internal reflections, which was ensured by making the samples slightly wedge shaped.

TABLE I. Constants used to calculate the absorption constant α and reflectance R.

Resonant absorption frequency[a] at 2 °K	ω_0	318 cm^{-1}
Static dielectric constant[a] at 2 °K	ϵ_0	8.5
High-frequency dielectric constant[a] at 2 °K	ϵ_∞	1.933
Szigeti effective charge[b]	e^*	0.8
Unit-cell volume	v	16.35×10^{-24} cm^3

[a]See Ref. 6. [b]See Refs. 11 and 12.

After α_{pure} and α_{imp} have been calculated from Eq. (1), the absorption coefficient α_{iso} due to the isotope-induced one-phonon processes may be obtained by subtracting α_{pure} from α_{imp}. This is more accurate than the common practice of calculating α_{iso} from the logarithmic ratio of the intensities transmitted by equal-thickness pure and impure samples. This latter ignores the denominator in Eq. (1), which, for example (in the case of LiF at 250 cm^{-1} where $R\sim0.4$, $\alpha_{pure}\sim0$, and $\alpha_{imp}d$ is the optimum value of 1), gives a 14% error in α_{iso}. (It is also not clear whether in Ref. 2 an isotopically pure sample was used to give the two-phonon summation background, which could be appreciable by 160 cm^{-1} in NaCl.)

The reflectance calculated from Eqs. (2) and (3) may been seen in Fig. 1, where the 7.5 °K measurements of Jasperse *et al.*[7] are included for comparison. Deviations up to 4% may be observed.

The solid lines in Fig. 2 are the measured values of α_{iso} and α_{pure} (the latter are included for interest) plotted on a logarithmic scale. The main feature in α_{iso}, which stands out more clearly on a linear plot, is the peak at (253 ± 1) cm^{-1}. A much smaller but definite feature was found at (282 ± 1) cm^{-1}. Despite the large uncertainty in the high-α measurements around 300 cm^{-1}, resulting from the poor resolution and signal-to-noise ratio, an indication of a change in slope in that region was also obtained. (At 300 cm^{-1} the reflectance is 0.6, which reduces the signal to a maximum of 25% of the incident intensity.) The error bars at 282 and 253 cm^{-1} resulted from two sources. The first and minor one was a 2% error assigned to d from the sample wedge shape and alignment accuracy. The second and larger source of error stemmed from the reflectances. If the reflectances from the pure and impure samples had been the same but differed from the calculated value by a few percent, as in Fig. 1, then the method used to calculate α_{iso} would have reduced the resulting error in α_{iso} to a very small percentage. However, evidence was found, from matching α_{iso} obtained from different thickness samples, that the reflectances from the pure- and impure-sample surfaces differed in some regions by as much as 5%. This is presumably due to the different polishing procedures. An error of 5% in R affects I and therefore $e^{-\alpha d}$ by approximately 10%, giving an error of ±0.1 in αd. The optimum value of αd for the best signal-to-noise ratio may be shown to be 1.0, giving a 10% error in α. For lower wave numbers, however, where αd for the thickest sample approached 0.1, the same error in R would pro-

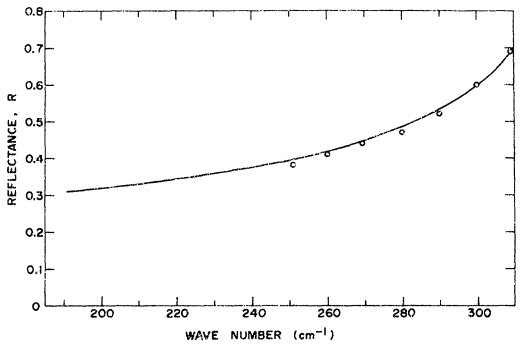

FIG. 1. Solid line represents the reflectance of LiF calculated as in the text. The open circles are the 7.5 °K experimental results of Jasperse *et al.*

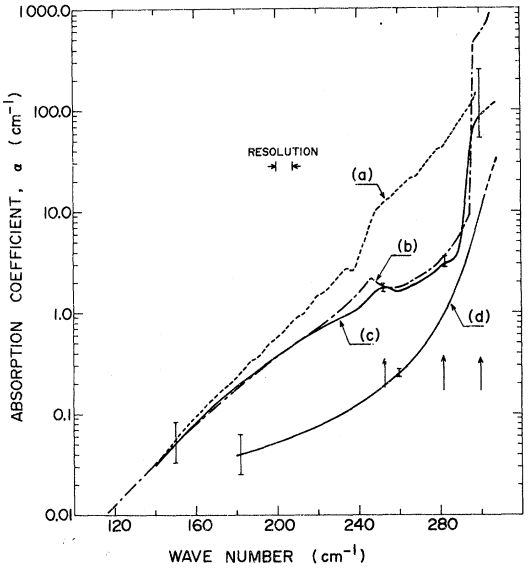

FIG. 2. Curve (a): predicted absorption using the deformation-dipole data of Karo and Hardy. Curve (b): predicted absorption using the shell-model data of Dolling *et al.* Curve (c): experimental values of the isotope-induced one-phonon absorption in natural LiF. The arrows mark the main features. Curve (d): experimental values of the low-energy tail of the two-phonon sum processes in pure Li^7F.

duce a 100% error in α. In these regions the noise was also about 50% of the signal.

III. THEORY AND CALCULATIONS

The theory outlined by Macdonald *et al.*[2] for the absorption produced by a large concentration of weakly perturbing isotopic mass defects predicts for the absorption constant

$$\alpha(\omega)=\frac{e_t^{*2}\,2\pi^2\omega^4\,\rho^+(\omega)}{n(\omega)cM_+^3v(\omega_0^2-\omega^2)^2}\,\langle(\Delta M_+)^2\rangle, \tag{4}$$

where e_t^* is the macroscopic effective charge associated with the transverse optic mode near $\vec{k}=0$, taken as

$$e_t^*=\tfrac{1}{3}e^*(n_\infty^2+2), \tag{5}$$

where e^* is the Szigeti effective charge, n is the refractive index, c is the velocity of light, v is the volume of the unit cell containing two atoms, M_+ is the average mass of the Li ions in the crystal, ΔM_+ is the deviation at a particular site of the Li-ion mass from M_+, and $\rho^+(\omega)$ is the phonon density of states for the Li sublattice, given by

$$\rho^+(\omega)=[\sum_{\vec{k},j}|\vec{m}^+(\vec{k},j)|^2\,\delta(\omega_{\vec{k},j}-\omega)]/[\sum_{\vec{k},j}|\vec{m}^+(\vec{k},j)|^2], \tag{6}$$

where $m^+(\vec{k},j)$ is the eigenvector of the Li ion associated with the phonon of wave vector $\vec{k}$ and branch index j. $\rho^+(\omega)$ is normalized such that

$$\int_0^\infty \rho^+(\omega)\,d\omega=1\ . \tag{7}$$

The absorption constant α was calculated from Eq. (4) using, first of all, the eigendata, kindly supplied by Karo and Hardy, obtained from a modified deformation-dipole model. The eigendata were supplied with a wave-vector grid corresponding to 64 000 $\vec{k}$ vectors per zone and the resulting $\alpha(\omega)$ values were smoothed by convoluting with a 25-point least-squares function[8] which gave a resolution of about 10 cm^{-1}. The values of the constants used in Eq. (4) may be seen in Table I. As has been found previously,[5] this model for LiF produces frequencies which differ appreciably from the neutron-measured values in some directions and the agreement with α in Fig. 2 may be seen to be poor.

Dolling *et al.*[4] generated weighted densities of state (frequency distribution curves) for the Li and F ions from their shell model, fitted to neutron-measured dispersion curves. Figure 6(b) of their paper shows a plot of $\rho^+(\omega)$ as defined in Eq. (6) but normalized so that the area equals $1/2M_+$ amu^{-1}. This plot is reproduced in Fig. 3, where the $\rho^+(\omega)$ units are cm instead of tera Hz^{-1}. The deformation-dipole density is included for comparison. Using the low-wave-number Dolling values from Fig. 3, the absorption constant was again calculated and may be seen in Fig. 2. The over-all agreement appears to be extemely good, including the feature near 250 cm^{-1} and the change of slope near 300 cm^{-1}. There is, however, a discrepancy in intensity near 250 cm^{-1} and no predicted feature near 280 cm^{-1}. Owing to the frequency shifting and distortion effect on maxima of the powerful $\omega^4/(\omega_0^2-\omega^2)^2$ term, the measured α values were converted to weighted Li-ion–phonon densities and may be seen together with the low-frequency region of Dolling's in Fig. 4.

The maximum at 251 ± 1 cm^{-1} (as opposed to 253 cm^{-1} in Fig. 2) is due to the transverse acoustic (TA) phonons at X_5' shifted down from the measured[4] room-temperature value of 257 ± 3 cm^{-1} for Li^7F. (The shell-model curve in Fig. 4 has its X_5' peak at 246 cm^{-1}.) A downward frequency shift, in this case 2–3%, with decreasing temperature is unusual but not unheard of.[9] The effect of the lighter-isotope impurity would also have been expected to increase, although admittedly only by a very small amount, rather than decrease the frequencies. The frequencies measured by Macdonald *et al.* in NaCl by this method were somewhat higher than the neutron values.[9]

The small feature at 282 cm^{-1} is difficult to assign. The next-highest major symmetry point after X_5' is W_1, which is forbidden by symmetry[10] because of the zero motion of the Li ion at that point. [Likewise L_1 and L_3 are forbidden, which explains the lack of any feature near 207 cm (measured L_3 wave number).] Possibly some flat region near Q or Z may be responsible, which did not exist in the shell-model calculation. [The Karo–Hardy combination of W_2' (380 cm^{-1}) + W_1 (290 cm^{-1}) equal to 670 cm^{-1} seemed to fare better than the shell-model combination (379 cm^{-1} + 271 cm^{-1}) equal to 650 cm^{-1} in comparison with a 670-cm^{-1} feature in the two-phonon conductivity.[5]] Certainly along the branch joining the forbidden points L_3 to W_1 the eigenvectors change to allow absorption and this may be the reason for the feature.

The weighted density of states predicted by the shell model appears to quickly deviate by up to 30% as the X_5' feature is approached. This implies a discrepancy of (15 ± 5)% in the shell-model acoustic lithium eigenvectors near the zone boundary. Such a discrepancy is not unusual, since Reid has found a variation from 0.7 to 1.1 in the quantity Γ defined by

$$\Gamma=|\vec{m}^+(\vec{k},j)|M_-^{1/2}/|\vec{m}^-(\vec{k},j)|M_+^{1/2}, \tag{8}$$

predicted by various models at the point X_5' for NaCl, with the variation increasing rapidly as the zone boundary is approached from a common value of 1 at the origin. The two eigenvectors at X_5' are

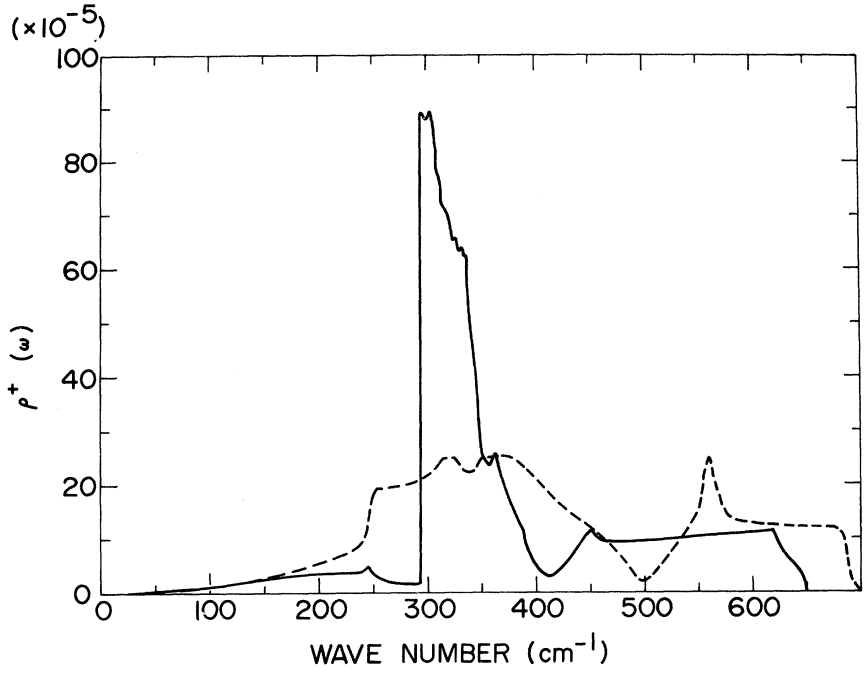

FIG. 3. Lithium-ion-phonon density of states predicted by the shell model of Dolling *et al.* (solid line) and by the modified deformation-dipole model of Karo and Hardy (dashed line). The area under each curve equals $(2M_+)^{-1}$ amu^{-1}. Units of $\rho^+(\omega)$ are cm.

parallel, perpendicular to the wave vector, and are normalized such that

$$m^+(\vec{k},j)^2 + m^-(\vec{k},j)^2 = 1. \tag{9}$$

Thus the variation found corresponds to a percentage variation of approximately 30% in the Na^+ eigenvector $m^+(\vec{k},j)$. Unfortunately, the peak values near 250 cm^{-1} in Fig. 4 cannot be used to calculate exactly the eigenvectors for the [100] TA mode at X_5' since there are contributions from

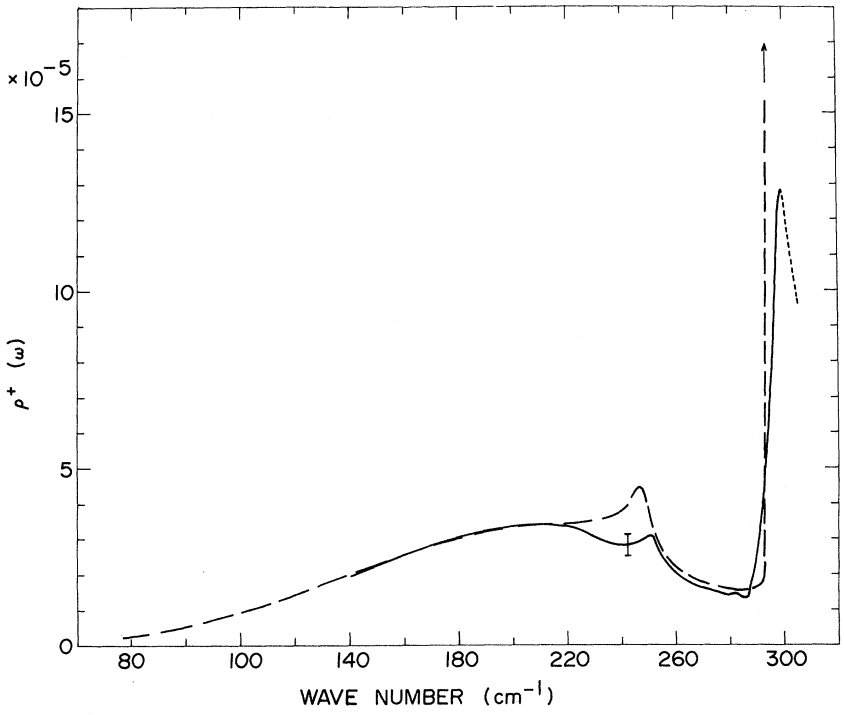

FIG. 4. Low-frequency region of the lithium-ion density of states of Dolling *et al.* (dashed line) and that calculated from the measured absorption coefficient (solid line). Units of $\rho^+(\omega)$ are cm.

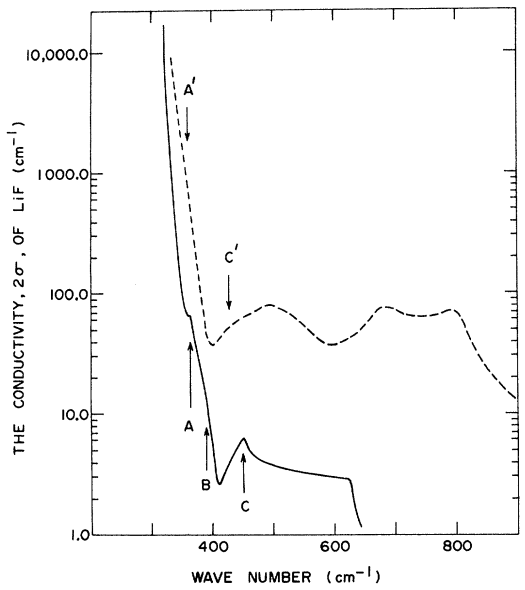

FIG. 5. Measured LiF conductivity above the reststrahlen frequency (dashed curve) with the calculated isotope-induced one-phonon contribution to the conductivity (solid curve).

other acoustic modes at that wave number, and the precise shape and height of the peaks depend on the shape of the dispersion curve. Nevertheless, by considering the Karo–Hardy eigenvectors at X_5', which agree fairly well with the approximate shell-model values calculated from the peaks in the Li and F phonon density curves, and by using Eq. (9), it is found that a 15% error in $m^+(X_5')$ leads to only about a 3% error in $m^-(X_5')$.

The effect of temperature is not certain but the Karo–Hardy data predict a small *decrease* of $m^+(X_5')$ going from 0 °K to room temperature for LiF, as also does the 1FRSM model for NaCl.[3] Another uncertain factor, the Szigeti effective charge, has been taken as 0.8 as used by Karo and Hardy,[11] in agreement with the value of 0.81 found by Martin.[12] This would seem to be reasonable considering the excellent agreement from 140 to 220 cm^{-1}.

IV. CONDUCTIVITY ABOVE RESTSTRAHLEN FREQUENCY

Since the agreement between the measured absorption constant α and that calculated from the shell-model data below the reststrahlen frequency ω_0 was very good, it was decided to use the theoretical data above ω_0 to calculate the contribution of the isotope-induced one-phonon processes to the conductivity measured by Smart, Wilkinson, Karo, and Hardy.[13] In Ref. 13 the conductivity was assumed to be due totally to two-phonon (or possibly multiphonon) summation processes, and a comparison was made with a calculated combined-density-of-states curve. Recently this author[5] used the same Karo–Hardy data as have been used here, and a more detailed theory to calculate the two-phonon-summation conductivity. The theory included cubic coupling coefficients which coupled the TO mode near $k=0$ to two other modes with equal but opposite wave vectors. By considering three simple criteria involving dispersion-curve slope matching, eigenvector polarization, and a sine-modulation term, it was found possible to assign all of the major and some of the minor features to specific phonon pairs. The frequencies of these pairs were taken from the neutron measurements.[4] One feature at 400 cm^{-1}, reported in Ref. 13 but so small as not to be seen in the published curve, could not be explained. In Fig. 5 may be seen this published curve together with the value of 2σ [equal to $n\alpha/2\pi$, thus canceling the n, which cannot be calculated from a classical formula above ω_0, in Eq. (4)] calculated using the weighted lithium-ion density-of-states values of Dolling *et al.*

The feature near 360 cm^{-1}, marked A in the one-phonon curve, presumably due to X_2' [longitudinal acoustic (LA)] and X_5'(TO), constitutes just under 10% of the measured curve and may be responsible for the slight change in slope just discernible in the published experimental curve of 2σ. Likewise, the feature seen at 400 cm^{-1} may be due to the change in slope of the one-phonon curve marked B, as L_1, a forbidden point, is approached. Thirty percent of the measured α at that point may be due to one-phonon processes. At C, a peak corresponding to X_2' [longitudinal optic (LO)], is about 10% of the measured 2σ and may be causing the slight mound labeled C'. The one-phonon intensity at 620 cm^{-1} just before the steep dropoff constitutes only about 6% of the measured curve and may therefore be difficult to observe.

V. CONCLUSION

The far-infrared isotope-induced one-phonon absorption in natural lithium fluoride has been measured with fair accuracy. This latter could be greatly improved with the use of a more sensitive detector, which would increase the signal-to-noise ratio where the absorption is weak and the resolution where the absorption is sharply rising. A better detector would also allow narrower collimating slits, thus reducing any possible divergence effects which may occur with the thick samples. Greater accuracy in the reflectance values for both the pure and impure samples would also be required.

Agreement with the theory given by Macdonald *et al.*,[2] using the shell-model lattice-dynamical data of Dolling *et al.*,[4] is over-all excellent but indicates a possible discrepancy of (15 ± 5)% in the lithium-ion eigenvectors near the zone boundary of

the [100] TA mode. This would imply only a 3% error or so in the corresponding fluorine-ion eigenvectors. As a method for checking these eigenvectors, isotope-induced absorption is very sensitive but allows access to only a few modes. Others are forbidden by symmetry or swamped by two-phonon summation absorption.

The frequency of the X_5' symmetry point has been found to decrease by 2–3% from the room-temperature value measured in Li^7F, opposite to the shift direction normally expected.

Finally, by using the shell-model data in the region above the reststrahlen frequency, it has been shown that the isotope-induced absorption may be responsible for some of the small features in the high values of conductivity measured by other authors.

ACKNOWLEDGMENTS

The author wishes to thank Professor A. M. Karo for kindly providing his lattice-dynamical data and Professor J. E. Bertie for a copy of his Fourier-analysis program.

†Work supported in part by the National Research Council of Canada under Grant No. 67-5653 and in part by the Defence Research Board of Canada under Grant No. 9510-35.

[1]See A. J. Sievers, in K. D. Möller and W. E. Rothschild, *Far-Infrared Spectroscopy*, (Wiley, New York, 1971), Appendix I.

[2]H. F. Macdonald, Miles V. Klein, and T. P. Martin, Phys. Rev. 177, 1292 (1969).

[3]J. S. Reid, Phys. Status Solidi 48, 591 (1971).

[4]G. Dolling, H. E. Smith, R. M. Nicklow, P. R. Vijayaraghavan, and M. K. Wilkinson, Phys. Rev. 168, 970 (1968).

[5]J. E. Eldridge, Phys. Rev. B 6, 1510 (1972).

[6]R. P. Lowndes and D. H. Martin, Proc. Roy. Soc. (London) 308, 473 (1969).

[7]J. R. Jasperse, A. Kahan, and J. N. Plendl, Phys. Rev. 146, 526 (1966).

[8]Abraham Savitsky and Marcel J. E. Golay, Anal. Chem. 36, 1627 (1964).

[9]G. Raunio, L. Almquist, and R. Stedman, Phys. Rev. 178, 1496 (1969).

[10]R. Loudon, Proc. Phys. Soc. (London) 84, 379 (1964).

[11]A. M. Karo and J. R. Hardy, Phys. Rev. 129, 2024 (1963).

[12]D. H. Martin, Advan. Phys. 14, 39 (1965).

[13]C. Smart, G. P. Wilkinson, A. M. Karo, and J. R. Hardy, in *Lattice Dynamics*, edited by R. F. Wallis (Pergamon, New York, 1965), p. 387.

PHYSICAL REVIEW B VOLUME 6, NUMBER 8 15 OCTOBER 1972

Thomas–Fermi Calculation of the Interlayer Force in Graphite*

Emilio Santos and Antonio Villagrá
Facultad de Ciencias, Universidad de Valladolid, Valladolid, Spain
and Grupo Interuniversitario de Física Teórica, Spain
(Received 21 January 1972)

A model of a graphite crystal is proposed in which planar layers of positive charge are considered instead of the point charges of nuclei. The interlayer electronic density is calculated integrating both the Thomas–Fermi and the Thomas–Fermi–Dirac equations. From these densities, the total energy of the electrons is calculated including corrections for inhomogeneity in the form of Weizsäcker and Kirzhnits. The influence of the different corrections is studied with the result that the best method is to calculate the density from the Thomas–Fermi–Dirac equation and to take into account the inhomogeneity corrections in the form of Kirzhnits.

I. INTRODUCTION

The method of Thomas–Fermi–Dirac (TFD) gives the energy of an electron system by means of the integral[1]

$$U=\int dv\left[\frac{3\pi^2\hbar^2}{10m}\left(\frac{3}{\pi}\right)^{2/3}\rho^{5/3}+\frac{\vec{E}^2}{8\pi}-\frac{3e^2}{4}\left(\frac{3}{\pi}\right)^{1/3}\rho^{4/3}\right], \tag{1}$$

where $\hbar$ is the reduced Planck constant, m is the electron mass and $-e$ its charge, ρ is the number of electrons per unit volume, and $\vec{E}$ is the electric field. The first term of the integral gives the kinetic energy of the electrons, the second one gives the potential energy, and the last one gives the exchange energy. The potential energy is given in terms of the electric field for later convenience. The integral (1) must be a minimum subject to the following conditions: the Poisson equation, which relates the electrostatic potential to the charge density, the normalization of the density, and the boundary conditions. The latter are usually stated by giving the positions of the external charges or